

Figure S1

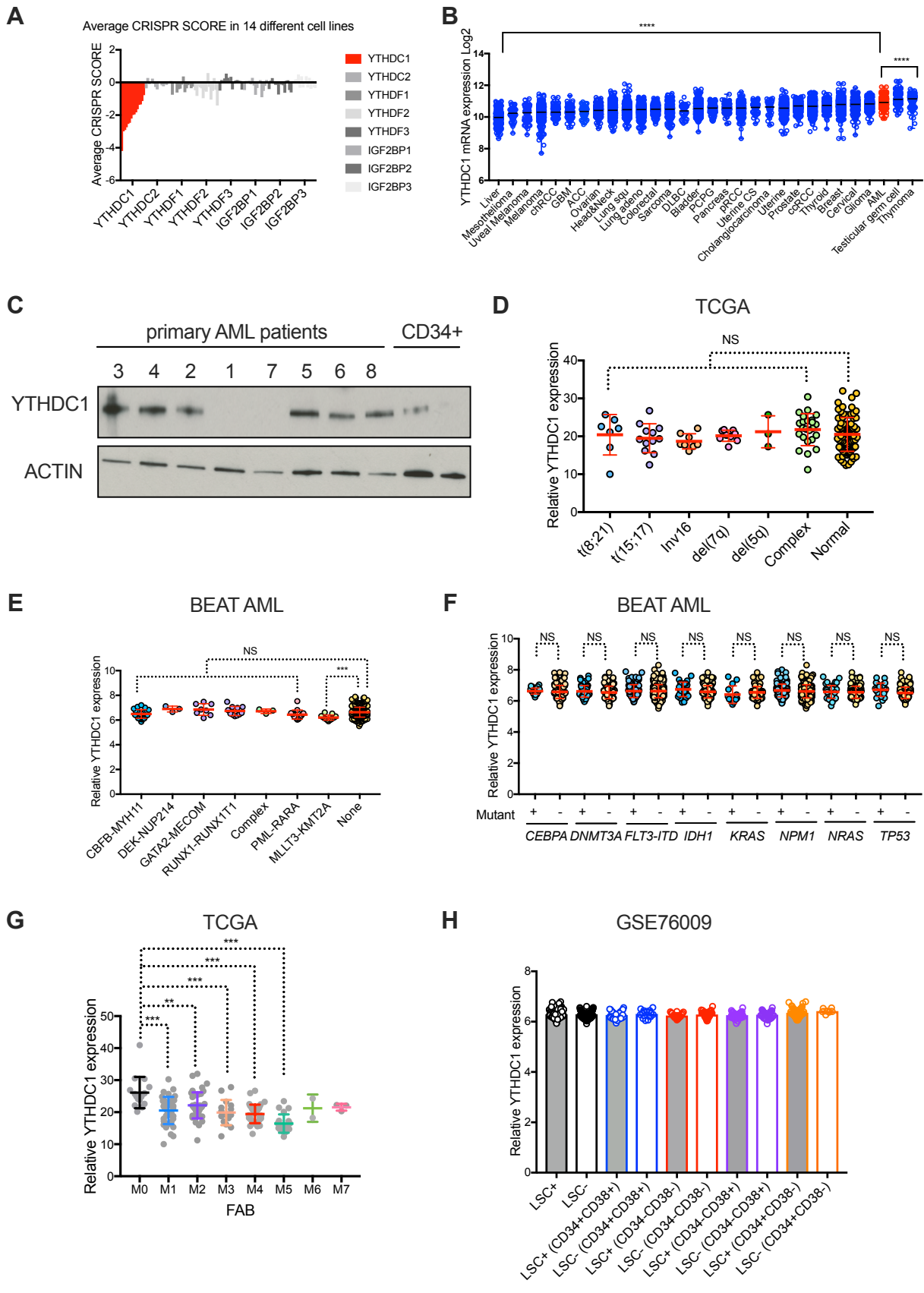


Figure S1: YTHDC1 is highly expressed in AML cells, Related to Figure 1.

(A) CRISPR score of m⁶A readers across all 14 tested leukemia cell lines.

(B) *YTHDC1* mRNA expression in acute myeloid leukemia (AML) compared to other cancers (The Cancer Genome Atlas database). Data are presented as mean log₂ expression with range. AML: red dots, **** p<0.00001 ANOVA with multiple comparisons.

(C) Immunoblot analysis of *YTHDC1* protein expression in primary AML patient cells compared to human CD34+ cells. ACTIN serves as loading control.

(D) *YTHDC1* mRNA expression across AML patients with different karyotype from TCGA database.

(E) *YTHDC1* mRNA expression across different subtypes of AML patients by WHO classification from BEAT AML database.

(F) *YTHDC1* mRNA expression in AML patients with or without indicated gene mutants from BEAT AML database.

(G) *YTHDC1* mRNA expression across different phases of AML patients by FAB classification (French-American-British) from TCGA database.

(H) *YTHDC1* mRNA expression in leukemia stem cells (LSC) versus non-LSCs from GSE76009.

Error bars, s.e.m. * p<0.05, **p<0.01, ***p<0.001, two-tailed t test.

Figure S2

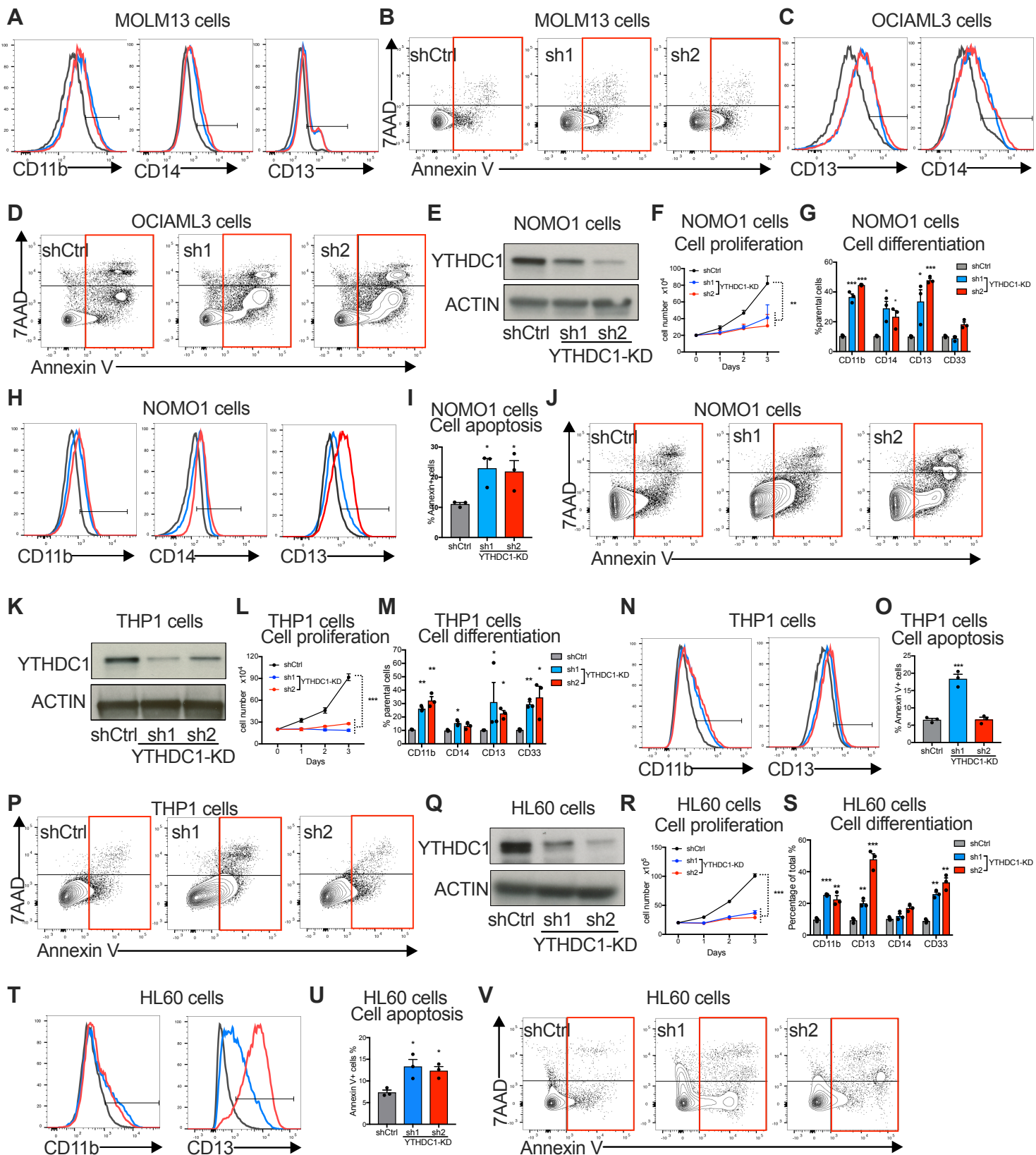


Figure S2: YTHDC1 is required for AML cell survival and state maintenance, Related to Figure 1.

(A) Representative flow plot to show CD11b, CD14 and CD13 expression in control and YTHDC1 knockdown MOLM13 cells 5 days after transduction related to **Figure 1G**.

(B) Representative flow plot to show cell apoptosis of control and YTHDC1 depleted MOLM13 cells in **Figure 1H**.

(C) Representative flow plot to show CD13 and CD14 in control and YTHDC1 knockdown OCIAML3 cells 5 days after transduction in **Figure 1K**.

(D) Representative flow plot to show cell apoptosis of control YTHDC1 depleted OCIAML3 cells in **Figure 1L**.

(E-V) YTHDC1 depletion by shRNAs in multiple AML cell lines.

(E-J) YTHDC1 is depleted in NOMO1 cells by shRNAs.

(E) Immunoblot of YTHDC1 expression post-transduction with shRNA lentiviruses in NOMO1 cells.

(F) Cell proliferation of NOMO1 cells upon YTHDC1 depletion was determined.

(G) Quantitative summary of myeloid differentiation in control and YTHDC1 depleted NOMO1 cells by flow cytometry in (H).

(H) Representative flow plot to show expression of myeloid differentiation markers in control and YTHDC1 knockdown cells in (G).

(I) Quantitative summary of cell apoptosis in NOMO1 cells determined by flow cytometry using 7-AAD and Annexin V staining.

(J) Representative flow plot to show cell apoptosis in control and YTHDC1 knockdown cells in (I).

(K-P) YTHDC1 is depleted in THP1 cells by shRNAs.

(K) Immunoblot of YTHDC1 expression post-transduction with shRNA lentivirus in THP1 cells.

(L) Cell proliferation of THP1 cells upon YTHDC1 depletion was quantified.

(M) Quantitative summary of myeloid differentiation following YTHDC1 depletion in THP1 cells.

(N) Representative flow plot to show expression of myeloid differentiation markers in control and YTHDC1 knockdown cells in **(M)**.

(O) Quantitative summary of cell apoptosis in THP1 cells determined by flow cytometry using 7-AAD and Annexin V staining.

(P) Representative flow plot to show cell apoptosis in control and YTHDC1 knockdown THP1 cells in **(O)**.

(Q-V) YTHDC1 is depleted in HL60 cells by shRNAs.

(Q) Immunoblot of YTHDC1 expression in HL60 cells post-transduction.

(R) Cell proliferation of HL60 cells upon YTHDC1 depletion was determined.

(S) Quantitative summary of myeloid differentiation in **(T)**.

(T) Representative flow plot to show expression of myeloid differentiation markers in control and YTHDC1 knockdown HL60 cells.

(U) Quantitative summary of cell apoptosis in HL60 cells determined by flow cytometry using 7-AAD and Annexin V staining.

(V) Representative flow plot to show cell apoptosis in **(U)**.

n=3 independent experiments; error bars, s.e.m. * p<0.05, **p<0.01, ***p<0.001, two-tailed t test.

Figure S3

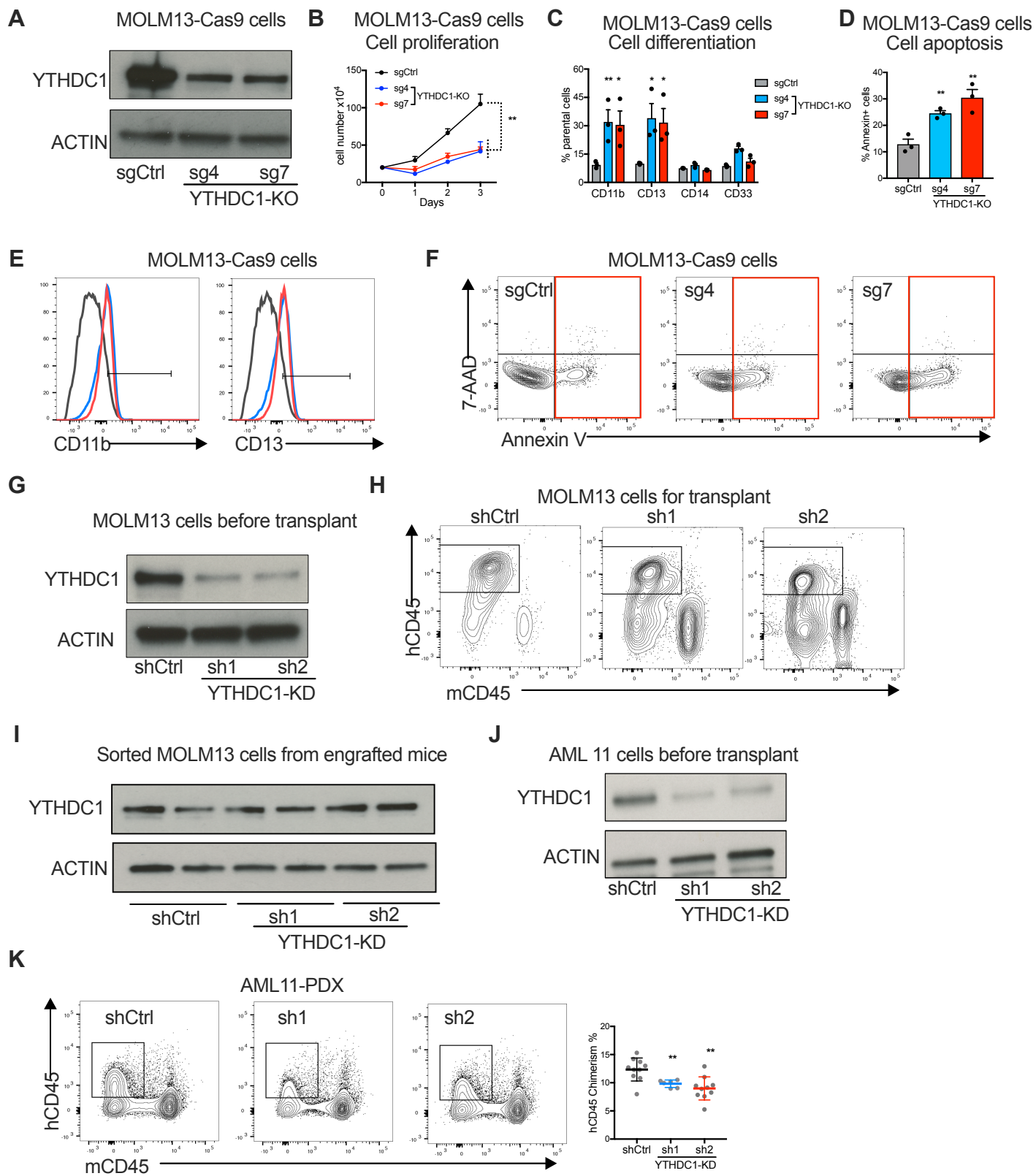


Figure S3: YTHDC1 maintains AML cell survival in vitro and in vivo, Related to Figure 1.

(A-F) CRISPR-Cas9 mediated-deletion of YTHDC1 in MOLM13 cells. MOLM13-Cas9 cells were transduced with lentiviruses expressing either a control sgRNA(sgCtrl) or two independent sgRNAs targeting YTHDC1 (sg4 and sg7). GFP positive cells were sorted. n=3 independent replicants.

(A) Immunoblot showing YTHDC1 expression in MOLM13 cells upon CRISPR-Cas9 mediated deletion. ACTIN serves as loading control.

(B) Cell proliferation of MOLM13 control cells versus CRISPR mediated YTHDC1 depleted cells.

(C) Quantitative summary of myeloid differentiation of MOLM13 cells post transduction was measured by flow cytometry using CD11b, CD33, CD13 and CD14 markers.

(D) Cells were assayed for Annexin V positivity measuring cell apoptosis.

(E) Representative flow plot to show expression of myeloid differentiation markers in MOLM13-Cas9 cells in (C).

(F) Representative flow plot to show cell apoptosis in (D).

(G) Immunoblot of YTHDC1 expression in MOLM13 cells before transplant into NSG mice.

(H) Representative flow plot to show engraftment of MOLM13 cells that injected into NSG mice in **Figure 1M**.

(I) Immunoblot analysis of MOLM13 *YTHDC1* knockdown cells that outgrow in moribund leukemic mice. Leukemia cells were sorted for human CD45 positive (a marker for hematopoietic cells) from leukemic mice in **Figure 1M**. ACTIN servers as loading control.

(J) Immunoblot of YTHDC1 expression in human AML11 cells before transplant into NSG mice.

(K) Left: Representative flow plot to show engraftment of AML11 cells that injected into NSG mice. Right: Quantitative summary of AML cell engraftment in NSG mice. n=10, n=7, n=10.

Error bars, s.e.m. * $p < 0.05$, ** $p < 0.01$, *** $p < 0.001$, two-tailed t test.

Figure S4: YTHDC1 forms nYACs that are involved in RNA processing, Related to Figure 2.

(A) Schematic representation of domains and disordered regions of human YTHDFs and YTHDC1 protein. Pink boxes indicate the YTH domain and the green shade indicate IDR.

(B) Sequence alignment of human YTHDF1, YTHDF2, YTHDF3, and YTHDC1 proteins. The YTHDF1 (UniProt Q9BYJ9), YTHDF2 (UniProt Q9Y5A9), and YTHDF3 (UniProt Q7Z739) share 50%-60% identity in their IDR domains while YTHDC1 (Q96MU7) does not show apparent sequence homology with the YTHDF proteins. In contrast, YTHDC1 owns four compositional bias regions (172 – 260: Glu-rich, 508 – 581: Arg-rich, 601 – 643: Pro-rich, 647 – 727: Arg-rich region) that are indicated by magenta lines. The blue line indicates the YTH domains. Conserved residues are highlighted in red and similar residues are highlighted in yellow. The residue numbers accounting for the YTHDF1 are denoted above the sequences. The alignment was performed by multAlin (<http://multalin.toulouse.inra.fr/multalin/>) and visualized with the ENDscript3.0 server (<https://academic.oup.com/nar/article/42/W1/W320/2435247>).

(C) Representative 3D Immunofluorescence (IF) images of YTHDC1 in CD34+, MOLM13, OCIAML3, HeLa, 293T and MCF7 cells showed nuclear YTHDC1 puncta. Fluorescence signal is shown as green for YTHDC1 and merged with DAPI stain (blue). Scale bars, 5 μ m.

(D) 106 YTHDC1 interacted proteins are from BIOGRID database and performed enrichment analysis by ENRICH.

(E) Representative 3D Immunofluorescence (IF) images of YTHDC1(green) costained with SRSF2, Coilin, PML, Brd4 and NPM1(magenta). DAPI is blue. Scale bars, 5 μ m

Figure S5

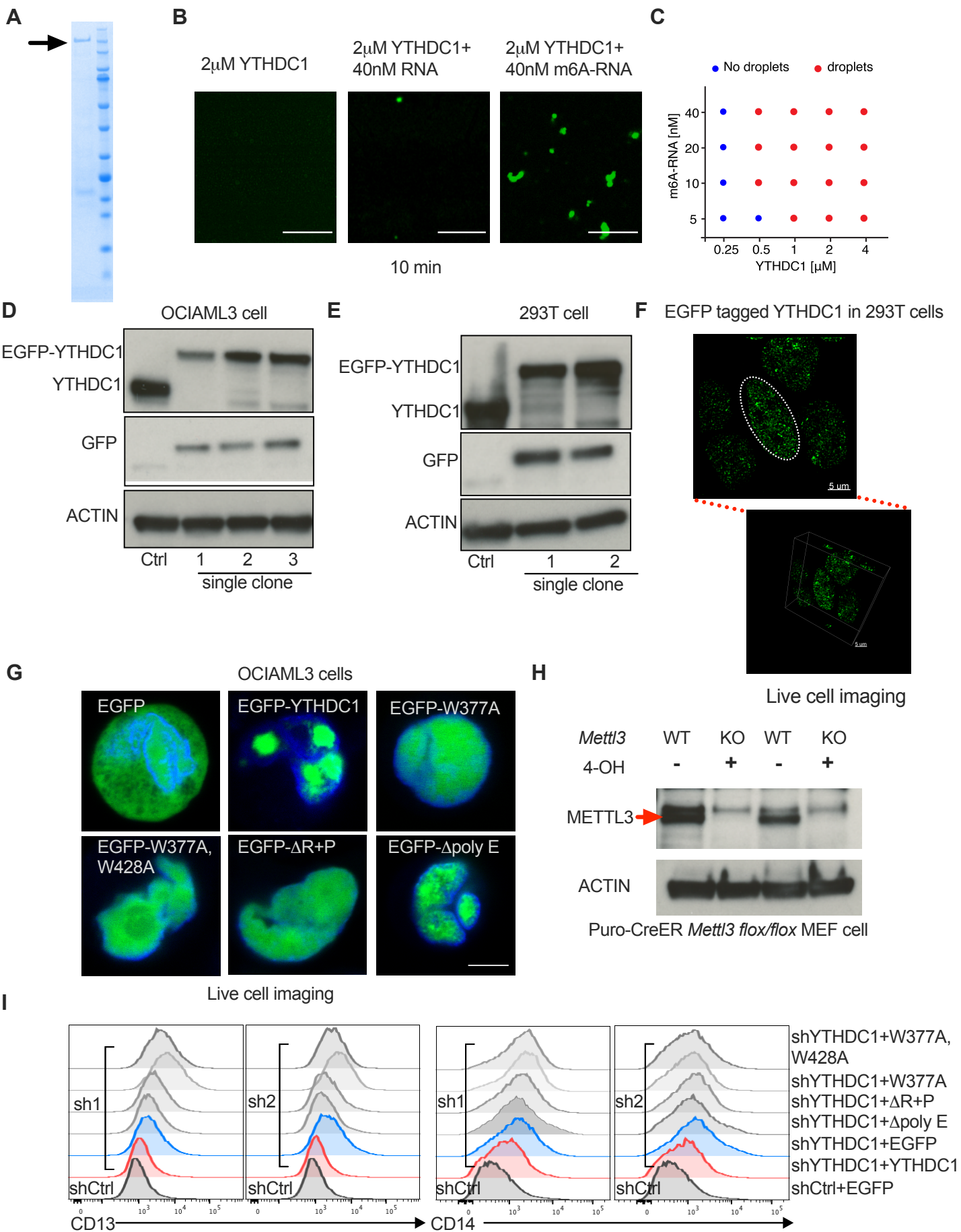


Figure S5: m⁶A dependent liquid-liquid phase separation of YTHDC1 *in vitro* and *in vivo*, Related to Figure 2 and 3.

(A) EGFP-YTHDC1 recombination protein was purified and confirmed by running a gel. Black arrow indicated the fusion protein band.

(B) A 65-nucleotide RNA containing 10 m⁶A nucleotides (40 nM) induces YTHDC1 (2μM) to rapidly form liquid droplets compared to YTHDC1 (2μM) protein without any RNA addition or with non- m⁶A RNA (40 nM) addition. Images were taken 10 minutes after RNA added.

(C) Phase diagram of YTHDC1 in the presence of different concentrations of m⁶A-RNA, showing that m⁶A-RNA dampens the phase-separation potential of the protein. Green dots indicate that protein droplets were present; blue dots indicate that no protein droplets were observed in the buffer.

(D) Confirmation of CRISPR-Cas9 knock in of EGFP-YTHDC1 in OCIAML3 cells. Immunoblot of YTHDC1 and GFP show endogenous expression of EGFP-YTHDC1 in different OCIAML3 clones compared to control cells.

(E) Confirmation of CRISPR-Cas9 knock in of EGFP-YTHDC1 in 293T cells. Immunoblot of YTHDC1 and GFP show endogenous expression of EGFP-YTHDC1 in different 293T clones compared to control cells.

(F) Live imaging of endogenously tagged EGFP-YTHDC1 in 293T cells showing YTHDC1 puncta. The white line highlights the nuclear periphery. Left: 2D image. Right: 3D image. Scale bars, 5μm.

(G) Live imaging of OCIAML3 cells expressing EGFP fused WT YTHDC1 and different YTHDC1 mutants as indicated. EGFP was used as control. Scale bars, 5μm.

(H) Immunoblot of METTL3 expression shows 4-OH induced METTL3 knockout in Puro-CreER transduced *Mettl3 flox/flox* MEF cells.

(I) Representative flow plot to show CD13 and CD14 expression in Figure 3J.

Figure S6

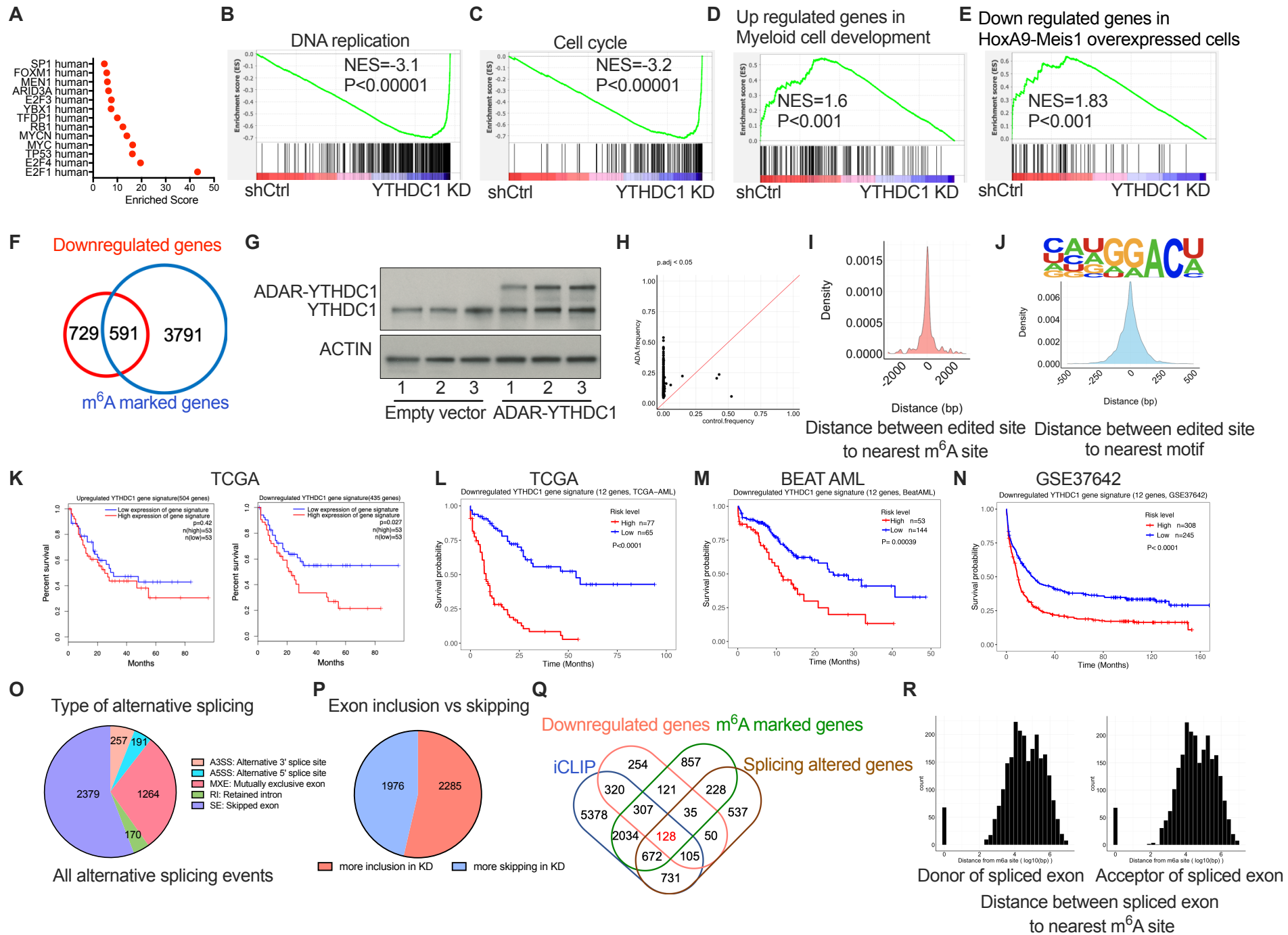


Figure S6: YTHDC1 depleted AML cells demonstrate a dysregulated gene expression program, Related to Figure 5.

(A) Transcription factors that enriched with downregulated genes upon YTHDC1 depletion were indicated.

(B-E) Unbiased gene set enrichment analysis using 4,733 curated gene sets against the rank list of differential expressed genes between control and YTHDC1 loss cells.

(B and C) Cell cycle and DNA replication signatures were negatively enriched in cells with YTHDC1 depletion.

(D and E) The gene sets promoting myeloid differentiation were enriched in YTHDC1 depleted cells.

(F) Overlap between downregulated genes in YTHDC1 depleted cells with genes containing at least 1 m⁶A site mapped by miCLIP.

(G-J) Hyper-TRIBE identifies YTHDC1 direct binding targets.

(G) Immunoblot of YTHDC1 expression to show overexpression of ADAR-YTHDC1 fusion protein in MOLM13 cells.

(H) Plot to show the edited frequency in ADAR-YTHDC1 expressed cells (Y axis) compared to control cells (X axis).

(I) The distance between ADAR-YTHDC1 edited sites to the closest m⁶A sites identified by miCLIP was plotted.

(J) Top: the most enriched motif found surrounding A-to-T editing sites in cells expressing ADAR-YTHDC1. Bottom: the distance between edited sites to nearest motif.

(K) Kaplan-Meier analysis of survival outcome in AML patients with low versus high expression of gene signature that is upregulated or downregulated upon YTHDC1 depletion. Data are from TCGA database.

(L) Kaplan-Meier analysis of survival outcome in AML patients with low versus

high expression of 12-genes signature of YTHDC1 direct regulated genes using LASSO-Cox regression model. Data are from TCGA database.

(M) Kaplan-Meier analysis of survival outcome in AML patients with low versus high expression of 12-genes signature of YTHDC1 direct regulated genes using LASSO-Cox regression model. Data are from BEATAML database.

(N) Kaplan-Meier analysis of survival outcome in AML patients with low versus high expression of 12-genes signature of YTHDC1 direct regulated genes using LASSO-Cox regression model. Data are from GSE37642 dataset.

(O) Pie diagram to show the percentage of different type of alternative splicing events. A3SS: alternative 3' splice site; A5SS: alternative 5' splice site; MXE: mutually exclusive exons; RI: retained intron; SE: splice exon.

(P) Pie diagram to show the percentage of inclusion and skipping of spliced exons upon YTHDC1 depletion.

(Q) Venn diagram shows overlapped genes 1: genes containing YTHDC1 binding sites identified by iCLIP; 2: downregulated genes upon YTHDC1 depletion. 3: genes containing at least 1 m⁶A site identified by miCLIP; 4: genes with splicing alteration in YTHDC1 depleted cells.

(R) The distance between both donor(left) and acceptor(right) of spliced exon to the closest m⁶A sites identified by miCLIP was determined.

Figure S7

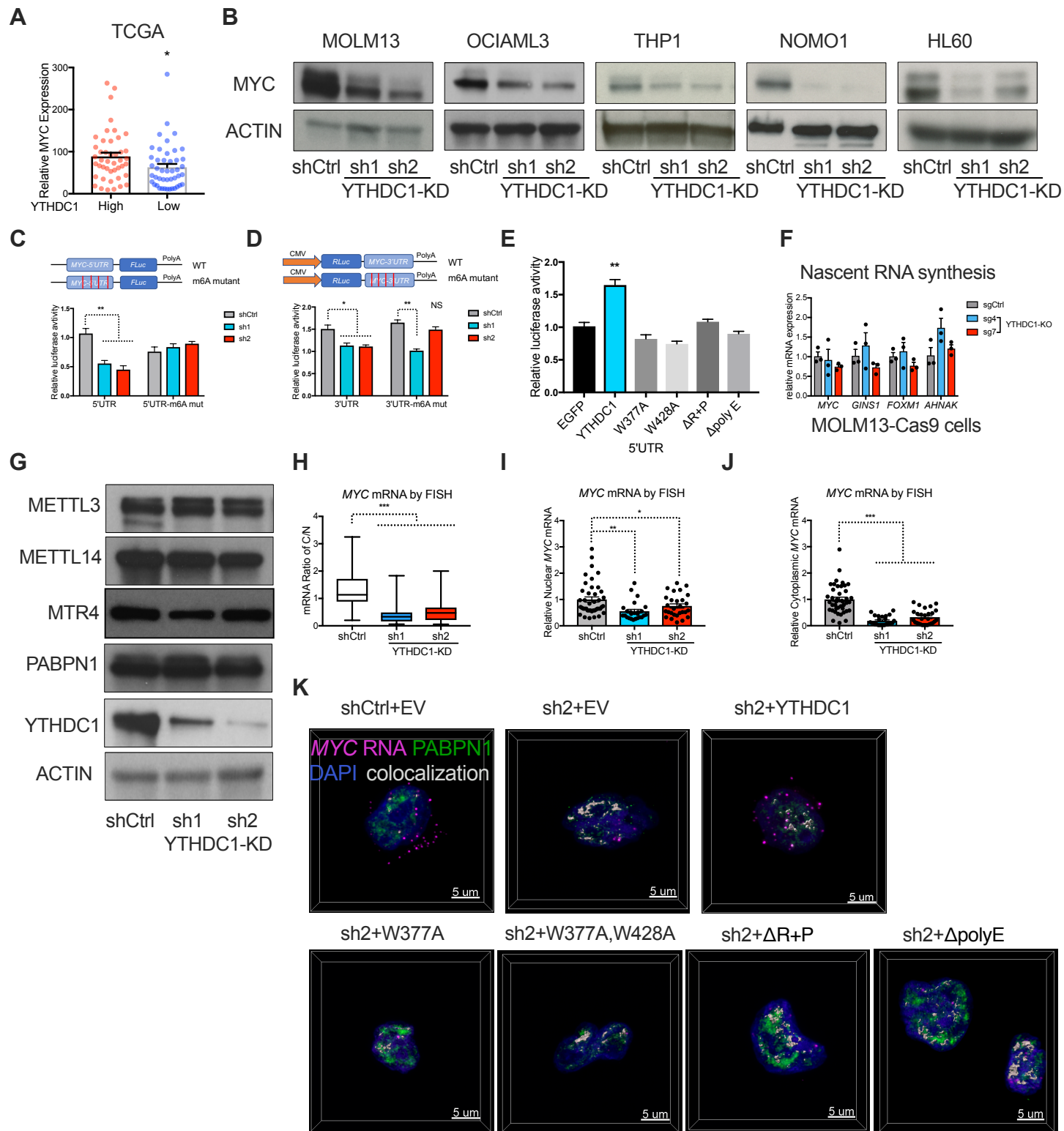


Figure S7: YTHDC1 regulates abundance of target transcripts by controlling mRNA stability, Related to Figure 6 and 7.

(A) *MYC* mRNA expression in AML patients with high versus low YTHDC1 expression from TCGA database.

(B) Immunoblot analysis of *MYC* protein abundance upon YTHDC1 knockdown by shRNAs in 5 AML cell lines as indicated. ACTIN serves as loading control.

(C) Up: Diagram of vector used in *MYC* 5'UTR luciferase reporter assay. Down: Luciferase reporter assay using the original *MYC* 5'UTR or the m⁶A sites mutated *MYC* 5'UTR in 293T cells. 293T cells were transfected with control or YTHDC1 shRNA constructs. Normalized luciferase activity was calculated as a ratio of Firefly/Renilla luciferase. n=4 independent experiments.

(D) Up: Diagram of vector used in *MYC* 3'UTR luciferase reporter assay. Down: Luciferase reporter assay using the original *MYC* 3'UTR or the m⁶A sites mutated *MYC* 3'UTR in 293T cells. 293T cells were transfected with control or YTHDC1 shRNA constructs. Normalized luciferase activity was calculated as a ratio of Renilla/ Firefly luciferase. n=4 independent experiments.

(E) Luciferase constructs are the same as **(C)**. 293T cells were transfected with control vector (EGFP), YTHDC1, or indicated YTHDC1 mutants. Normalized luciferase activity was calculated as a ratio of Firefly/Renilla luciferase. n=4 independent experiments.

(F) Analysis of nascent RNA synthesis of specific genes in control or YTHDC1 depleted MOLM13 cells by sgRNAs. *MYC*, *GINS1* and *FOXMI* are binding targets of YTHDC1 and downregulated in YTHDC1 depleted cells. *AHNAK* is one of top increased genes upon YTHDC1 depletion. Nascent RNA synthesis of specific genes was detected by using Nascent RNA Capture Kit following with qPCR.

(G) Immunoblot showing METTL3, METTL14, MTR4 and PABPN1 protein levels in control and YTHDC1 depleted MOLM13 cells. ACTIN serves as loading control.

(H) The nuclear to cytoplasm ratio of *MYC* mRNA was determined in control and YTHDC1 depleted MOLM13 cells by RNA-FISH. Nuclei that were defined using DAPI signal. Cytoplasmic signal was defined by subtracting nuclear region.

(I) Relative reduction of nuclear *MYC* mRNA in YTHDC1 depleted MOLM13 cells compared to control cells was determined by RNA-FISH.

(J) Relative reduction of cytoplasm *MYC* mRNA in YTHDC1 depleted MOLM13 cells compared to control cells was determined by RNA-FISH.

(K) OCIAML3 cells overexpressed with control, WT YTHDC1 or different YTHDC1 mutants as indicated were followed endogenous YTHDC1 knockdown by viral transduction. Representative 3D images of *MYC* mRNA by FISH (magenta) and fluorescence immunostaining of PABPN1 protein (green) and DAPI (blue) related to Fig. 7A and B to show co-localization between *MYC* mRNA and PABPN1 protein (white dots). Scale bars, 5 μ m.

Error bars, s.e.m. * $p < 0.05$, ** $p < 0.01$, *** $p < 0.001$, two-tailed t test.